Nucleation Mechanism of $YBa_2Cu_3O_{7-\delta}$ on $SrTiO_3(001)$

T. Haage, J. Zegenhagen,* H.-U. Habermeier, and M. Cardona
Max-Planck-Institut für Festkörperforschung, Heisenbergstrasse 1, D-70569 Stuttgart, Germany
(Received 1 December 1997)

Using UHV-scanning-tunneling microscopy and spectroscopy we show that submonolayer coverages of $YBa_2Cu_3O_{7-\delta}$ deposited on $SrTiO_3(001)$ nucleate as cubic, semiconducting $(Y, Ba)CuO_{3-x}$ phase as proven by the height of the nuclei and their density of states. Nuclei are observed at upper step edges and on the substrate terraces exclusively. Minimization of surface and interface energies forces this nucleation behavior. At about one monolayer, the film transforms into the orthorhombic, metallic $YBa_2Cu_3O_{7-\delta}$ phase indicating that the formation enthalpy of the bulk phases now dominates the growth process. [S0031-9007(98)06001-3]

PACS numbers: 68.35.Fx, 74.76.Bz, 82.65.–i

High-temperature superconducting (H-T_c) thin films are expected to play an important role in new classes of microwave and electronic devices. Thus, advances in the understanding of their nucleation and growth are of great technological interest. It is likewise of fundamental importance to gain a deeper understanding of the mechanism of the heteroepitaxial growth of multinary compound materials. In this Letter we present novel observations of the initial stages of the nucleation and growth of $R Ba_2Cu_3O_{7-\delta}$ (RBCO, R = rare earth) epitaxial thin films. We report here the results of a combined ultrahigh vacuum scanning tunneling microscopy (STM) and spectroscopy (STS) study of $YBa_2Cu_3O_{7-\delta}$ (YBCO) nucleation on carefully annealed and well-ordered $SrTiO_3(001)$ substrates without exposing the surface to air. For submonolayer coverage, we find building blocks of YBCO with different heights, typically 0.4 and 0.8 nm, and thus all smaller than the YBCO unit cell of 1.2 nm. The nucleation and growth occurs on the substrate terraces or at the upper edge of substrate steps but not at the bottom. The orthorhombic RBCO phase with $c = 1.2$ nm forms at coverages of around one monolayer (ML), i.e., at a thickness of about 1.2 nm.

Previous *ex situ* STM studies on more than 9 nm thick films grown by pulsed laser deposition (PLD) showed that the growth of YBCO on $SrTiO_3(001)$ generally proceeds layer by layer followed by the formation of islands (Stranski-Krastanov mechanism) [1]. Terashima *et al.* [2] reported oscillations in the intensity of the specular reflectivity of high-energy electrons during film growth by reactive evaporation. From these oscillations the growth unit was also inferred to be the complete unit cell of YBCO. Remarkably, non-unit-cell high growth steps have been discovered on YBCO films which had not been exposed to air prior to the STM investigation [3]. Thus, it is possible to force stoichiometric deposited YBCO material to assemble in smaller building blocks, yielding c-axis units different from the usual 1.2 nm high orthorhombic YBCO unit cell. Recent progress in the *in situ* preparation and characterization of $SrTiO_3$ surfaces allowed the utilization of tailored substrate surfaces for controlling the structure (and morphology) of YBCO thin films [4,5]. We have demonstrated how to manipulate in this way electronic transport and the concomitant flux pinning in superconducting YBCO films [5].

Little is known about the very initial nucleation of H-T_c films. In our first *in situ* study of the early stages of GdBCO growth by PLD we already observed non-unit-cell step heights [6]. A subsequent study of the nucleation of $SmBa_2Cu_3O_{7-\delta}$ on $SrTiO_3(001)$, grown by molecular beam epitaxy, *ex situ* by atomic force microscopy concluded that the films nucleate on the TiO_2 terminated surface exclusively as complete molecular units with the stacking sequence BaO-CuO_2-R-CuO_2-BaO-Cu-BaO at the bottom of substrate step edges [7]. However, Rutherford backscattering spectrometry studies proved that the outermost layer of an RBCO film exposed to air is chemically and structurally modified [8], a fact corroborated by our own observations. Our present study is aimed at lifting the controversies and providing a deeper understanding of the nucleation of YBCO on $SrTiO_3$ prior to the completion of the first ML.

The experiments were carried out in an ultrahigh vacuum (UHV) chamber with a base pressure of 5×10^{-11} mbar, interconnected with a PLD chamber. Slightly Nb-doped (0.02%) $SrTiO_3(001)$ substrates were annealed in UHV at a temperature of 950 °C for 2 h. This sufficed to generate clean and well-ordered surfaces, as judged by Auger electron spectroscopy and low-energy electron diffraction. The loss of oxygen during UHV annealing results in n-type conductivity which enables us to image the clean substrate surfaces of undoped samples by UHV-STM prior to deposition. Doped and undoped $SrTiO_3$ samples reveal the same well-ordered surface structure and morphology. Nb doping enables STM/STS measurements even after reoxidation during the RBCO deposition. Our STM achieves a resolution better than 0.01 nm vertically and 0.2 nm laterally on semiconductor surfaces. The STM scanner was calibrated with the 7×7 reconstruction of a Si(111) surface.

The YBCO films were grown by PLD at a substrate temperature of 750 °C in an oxygen atmosphere of 0.2 mbar, oxygenated (750 mbar O_2) immediately after deposition and cooled to 450 °C. The samples were kept at this temperature for 20 min and finally cooled to room temperature. Such YBCO films with a thickness of more than 120 nm exhibit a transition temperature of 90–91 K and a critical current density $>1 \times 10^{11}$ A/m^2 at 4.2 K [5]. The YBCO coverages were calibrated based on thickness measurements of relatively thick films. We define 1 ML of YBCO as a homogeneous layer with a thickness of 1.17 nm, i.e., the unit-cell height of YBCO.

After the growth process the deposition chamber was pumped to a pressure of less than 10^{-7} mbar and the samples were transferred to the UHV-STM stage without exposing them to air. All STM images were recorded in the constant current mode with tunneling currents of 0.2–0.3 nA and a sample bias of 0.75–1.9 V. The tunneling spectra were measured at room temperature for a grid pattern of points during frame scans [9]. Thus, we can inspect spectra for defined locations in the topographic image. For the selected spectra, the dynamic conductance dI/dU is numerically calculated and then normalized by the dc conductance I/U. This quantity $dI/dV/(I/V)$ corresponds closely to the local density of electronic states at the sample surface [10].

Prior to the YBCO deposition, the UHV-annealed substrate surface shows smooth terraces and a descending sequence of perfectly straight steps resulting from a vicinal off-cut [3° off (001) toward [010]] [11]. The topography of a $SrTiO_3$(001) surface after deposition of 0.5 (±0.1) ML YBCO is shown in Fig. 1. The underlying substrate surface with flat terraces and steps with a height of 0.8 or 1.2 nm [cf. Fig. 1(b)] and sharp edges can be distinguished. The deposited YBCO film forms islands, typically 14 nm wide and 70 nm long, on the $SrTiO_3$(001) terraces. The nuclei are aligned along the straight step edges and appear to nucleate preferentially on the upper edge of $SrTiO_3$ steps or occasionally freely on the terraces. A large number of STM images proves that none of the deposited material starts to grow from the bottom of the substrate steps. In the direction of the sample miscut we can distinguish up steps with a height of 0.4 and 0.8 nm associated with the YBCO islands [see Fig. 1(b)]. We have ruled out the possibility that the measured heights are somehow modified by a shadow effect of the STM tip since the $SrTiO_3$ steps are resolved sharply.

After deposition of 0.8 (±0.1) ML, the terrace structure associated with the clean substrate surface is still evident [see Fig. 2(a)]. The YBCO islands coalesce preferentially along the terraces whereas they are still discontinuous normal to the step edges leading to an anisotropic film morphology. Obviously, the steps represent effective diffusion barriers. The STM image in Fig. 2(a) shows islands, mostly ≈1.2 nm high. This height now equals the

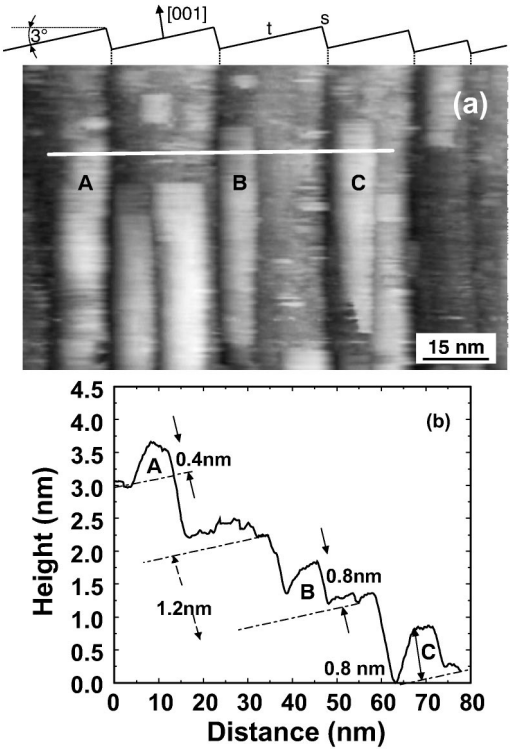

FIG. 1. (a) UHV-STM image (unfiltered raw data) of $SrTiO_3$(001) after deposition of 0.5 (±0.1) ML of YBCO. The $SrTiO_3$ crystal was cut 3° off (001) toward [010] leading to almost regularly spaced (001) terraces (t) separated by steps (s) as indicated on the top. (b) Cross section of the topography along the white line displayed in (a), crossing the three nuclei A, B, and C.

c axis length of YBCO. As an example, Fig. 2(b) shows a line profile across a partially covered $SrTiO_3$ terrace.

The observation of islands which do not have the height of a unit cell following the deposition of 0.5 (±0.1) ML implies that a phase different from $YBa_2Cu_3O_{7-\delta}$ forms at the very initial stage of growth. A typical STS spectrum taken at the surface of a 0.8 nm high island is shown in Fig. 3(a). The 0.5 eV wide gap in the local density of states reflects a semiconducting behavior of the non-unit-cell high clusters. It has been shown that under slightly modified growth conditions with a cation stoichiometry Y:Ba:Cu = 1:2:3 (or close to 1:2:3) films with a simple-cubic ABO_3 perovskite structure can be prepared. In this structure Y and Ba ions occupy the A sites with random distribution and Cu ions occupy the B sites [13,14]; i.e., the orthorhombic unit cell decomposes into perovskite-like, cubic subunits. The heights of the islands which we measured here equal integral multiples of the lattice constant $a_c = 0.3897$ [13] of this cubic structure. Moreover, the depression of the density of states around the Fermi level in the tunneling spectrum is in agreement with the semiconducting transport characteristics of the cubic Y-Ba-Cu-O material [13]. All this supports the assignment of the non-unit-cell high islands which appear at the very initial stage of growth to the cubic $(Y, Ba)CuO_{3-x}$ phase.

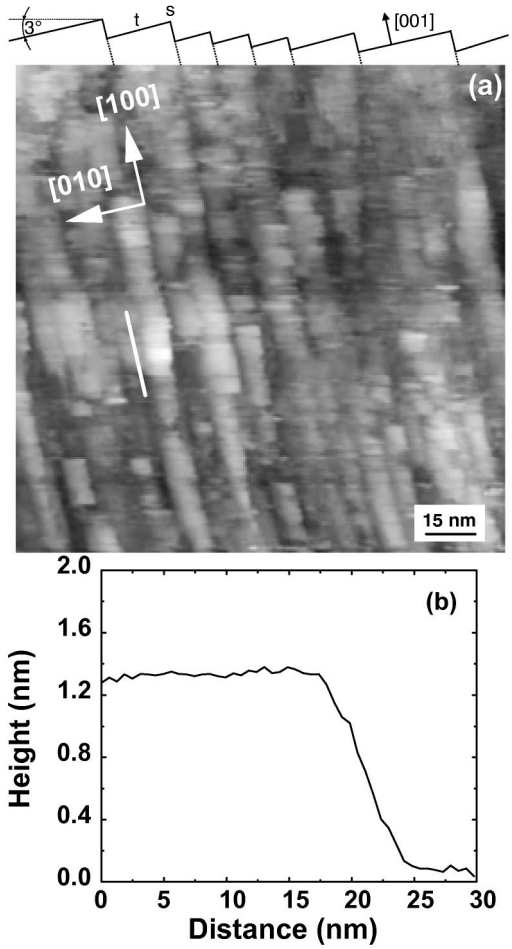

FIG. 2. (a) UHV-STM image (unfiltered raw data) of $SrTiO_3(001)$ after deposition of 0.8 (± 0.1) ML of YBCO. The terrace structure is indicated. The surface is almost completely covered with nuclei of varying size and not all step edges can clearly be distinguished. Note the larger scale compared to Fig. 1. (b) Cross section of the topography along the white line displayed in (a). Note the smaller horizontal scale.

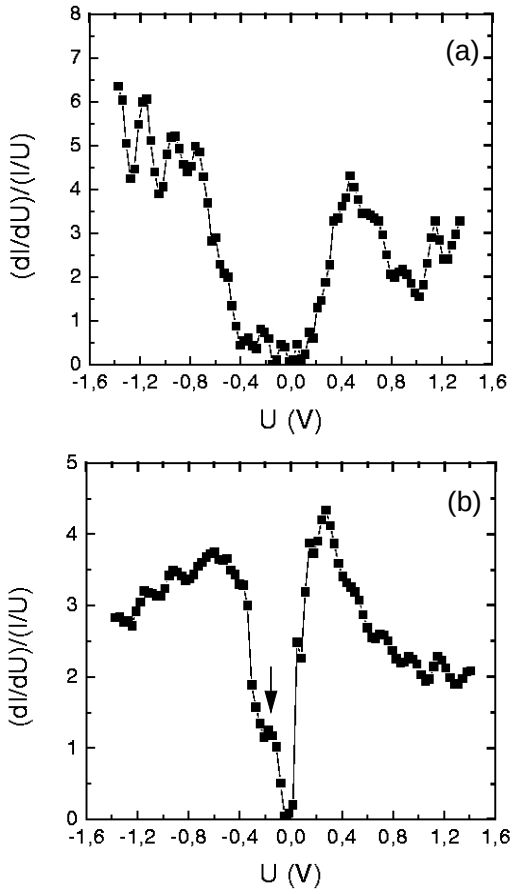

FIG. 3. (a) Normalized tunneling conductance $(dI/dV)/(I/V)$ vs applied bias V taken on the surface of (a) 0.8 and (b) 1.2 nm high islands appearing on a vicinal $SrTiO_3(001)$ surface after deposition of (a) 0.5 and (b) 0.8 ML of YBCO. The arrow in (b) marks a peak in the local electronic density of states that is referred to in the text.

STS measurements on the surface of 1.2 nm high islands [see Fig. 3(b)] show a different electronic structure. The gap around the Fermi surface appears to close as 1.2 nm high islands are formed, indicating a transition to a metallic phase. A similar STS spectrum also containing the marked peak in the local density of states at -0.15 eV has been found by Kawasaki *et al.* [15] on relatively thick YBCO films.

Our findings suggest that a critical volume of the deposited material is needed for spontaneuos nucleation of the YBCO structure on $SrTiO_3(001)$. The desired YBCO phase is formed at a coverage of more than 0.8 ML as individual islands coalesce and grow laterally and vertically, consuming the previously formed clusters.

However, the question arises as to what forces the formation of a different phase at the very first moments of nucleation and its transformation into the desired superconducting phase as deposition proceeds. We believe that most detrimental factors for the nucleation of the YBCO phase at small coverages are surface and interface energy contributions to the total energy. While the a/b plane of YBCO as well as the whole family of (001) planes of perovskites can exhibit nonpolar surfaces and, correspondingly, a comparably low surface energy, this is not the case for the a/c, b/c planes of RBCO which are exposed to a large extent in small clusters. Additionally, for small nuclei, edge and kink sites can strongly enhance the total energy. Simply minimizing the surface energy by adhering to the bottom of step edges is not possible for the YBCO phase since (a) $SrTiO_3(001)$ and YBCO step heights do not match and (b) there is generally a chemical and structural misfit at step edges as Fig. 4 schematically shows. Thus, for the YBCO phase to form, a certain critical volume of material is needed. A further contribution to the total energy comes from the interface energy. Here, the cubic phase is also favored since it exhibits only 0.3% mismatch with the $SrTiO_3$ in contrast to 1.5% (average between a and b axis) for the YBCO. Last but not least,

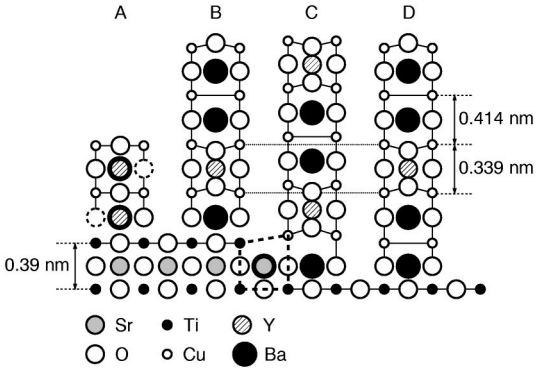

FIG. 4. Schematic model for the nucleation and growth of $R\mathrm{Ba_2Cu_3O_{7-\delta}}$ on Ti-terminated $\mathrm{SrTiO_3}(001)$. Nucleus of the random perovskite $(\mathrm{Y, Ba})\mathrm{Cu_{3-x}}$ (A), YBCO on upper step edge (B), YBCO on a terrace (C) which would experience a structural and chemical misfit if adhering directly to the bottom of the step as schematically indicated, and YBCO on the terrace with alternate stacking sequence (D) which achieves matching with YBCO (B) on the upper terrace.

while for the YBCO bulk phase to form the stoichiometry of the material supplied by the PLD is exactly correct, this is not the case for the first monolayer. The YBCO binds to the TiO_2 terminated surface via the BaO layer with two possible stacking sequences [16] as shown in Fig. 4. For either sequence the cation stoichiometry is *not* exactly 1:2:3. Thus, the surplus material must arrange on the surface in a different phase, also affecting the total energy of the system. In case of nucleation of the cubic perovskite phase (cf. Fig. 4), the cation stoichiometry can be (Y + Ba):Cu = 1:1, i.e., exactly as supplied. Since the deposition is performed in oxygen, the anion stoichiometry is adjusted easily.

For both the cubic phase and the YBCO phase, attaching to upper steps edges could reduce edge sites for the discontinuous films but it does not seem to be a way of reducing the total energy significantly since many nuclei grow freely on the terraces. It is interesting to note that as soon as the H-T_c film has reached a certain thickness, i.e., when the surface is completely overgrown and many of the defects originating from substrate step edges have been mended by insertion of stacking faults [5], step flow takes over in the growth of the films. As a result, smooth films without Stranski-Krastanov growth islands can be produced on $\mathrm{SrTiO_3}(001)$ surfaces with a moderate miscut [5].

In conclusion, we have provided clear evidence that the very first stage of nucleation of YBCO material on $\mathrm{SrTiO_3}(001)$ does not occur in the form of the H-T_c phase but as cubic, semiconducting perovskite. The main reasons for this are surface and interface energy contributions but the growth is also favored by the stoichiometry of the supplied cation material. At coverage close to 1 ML, as islands coalesce, the epitaxial layer transforms to the YBCO phase. Nucleation at up steps is avoided at the early stages of growth and step edges represent effective diffusion barriers causing pronounced anisotropies in the film structure in accordance with recent observations of anisotropic transport properties in films grown on vicinal surfaces.

This work was supported by the German BMBF Contract No. 13N5840 and the European Union Contracts No. EU CHRX-CT 94-0523 and No. EU CHRX-CT 930137.

*Corresponding author.
Electronic address: jorg@tunux2.mpi-stuttgart.mpg.de

[1] X.-Y. Zheng, D. H. Lowndes, S. Zhu, J. D. Budai, and R. J. Warmack, Phys. Rev. B **45**, 7584 (1992).
[2] T. Terashima, Y. Bando, K. Iijima, K. Yamamoto, K. Hirata, K. Hayashi, K. Kamigaki, and H. Terauchi, Phys. Rev. Lett. **65**, 2684 (1990).
[3] T. Haage, Q. D. Jiang, M. Cardona, H.-U. Habermeier, and J. Zegenhagen, Appl. Phys. Lett. **68**, 2427 (1996).
[4] T. Haage, H.-U. Habermeier, and J. Zegenhagen, Surf. Sci. **370**, L158 (1997).
[5] T. Haage, J. Zegenhagen, J. Q. Li, H.-U. Habermeier, M. Cardona, Ch. Jooss, R. Warthmann, A. Forkl, and H. Kronmüller, Phys. Rev. B **56**, 8404 (1997).
[6] Q. D. Jiang and J. Zegenhagen, Surf. Sci. **338**, L882 (1995).
[7] V. C. Matijasevic, B. Ilge, B. Stäuble-Pümpin, G. Rietveld, F. Tuinstra, and J. E. Mooij, Phys. Rev. Lett. **76**, 4765 (1996).
[8] D. Hüttner, O. Meyer, J. Reiner, and G. Linker, Appl. Phys. Lett. **66**, 1273 (1995).
[9] For a spectroscopy measurement the scan is halted, the sample-tip distance kept constant, and the tunneling current I measured as a function of voltage U (ranging from -1.6 to $+1.6$ V).
[10] R. M. Tromp, Z. Phys. **1**, 10 211 (1989).
[11] The structure of vicinal $\mathrm{SrTiO_3}(001)$ surfaces as revealed by UHV-STM has been described in detail in previous publications; see, e.g., [4,5,12].
[12] Q. D. Jiang and J. Zegenhagen, Surf. Sci. **367**, L42 (1996).
[13] J. A. Agostinelli, S. Chen, and G. Braunstein, Phys. Rev. B **43**, 11 396 (1991).
[14] A. Köhler, S. Linzen, J. Kräusslich, P. Seidel, B. Freitag, and W. Mader, Physica (Amsterdam) **282C–287C**, 571 (1997).
[15] M. Kawasaki and M. Nantoh, MRS Bull. **19**, 33 (1994).
[16] J. Zegenhagen, T. Siegrist, E. Fontes, L. E. Berman, and J. R. Patel, Solid State Commun. **93**, 763 (1995).